Protein and mRNA Expression in Uveal Melanoma Cell Lines Are Related to GNA and BAP1 Mutation Status

Maria Chiara Gelmi,[1] Arnoud H. de Ru,[2] Peter A. van Veelen,[2] Rayman T. N. Tjokrodirijo,[2] Marc-Henri Stern,[3] Alexandre Houy,[3] Robert M. Verdijk,[4,5] T. H. Khanh Vu,[1] Bruce R. Ksander,[6] Jolanda Vaarwater,[7,8] Emine Kilic,[8] Erwin Brosens,[7] and Martine J. Jager[1]

[1]Department of Ophthalmology, Leiden University Medical Center, Leiden, The Netherlands
[2]Center for Proteomics and Metabolomics, Leiden University Medical Center, Leiden, The Netherlands
[3]Inserm U830, DNA Repair and Uveal Melanoma (D.R.U.M.), Institut Curie, PSL Research University, Paris, France
[4]Department of Pathology, Ophthalmic Pathology Section, Erasmus MC, Rotterdam, The Netherlands
[5]Department of Pathology, Leiden University Medical Center, Leiden, The Netherlands
[6]Schepens Eye Research Institute, Massachusetts Eye and Ear Infirmary, Boston, Massachusetts, United States
[7]Department of Clinical Genetics, Erasmus MC Cancer Institute, Rotterdam, The Netherlands
[8]Department of Ophthalmology, Erasmus MC, Rotterdam, The Netherlands

Correspondence: T. H. Khanh Vu, Department of Ophthalmology, Leiden University Medical Center, P.O. Box 9600, Leiden 2300 RC, The Netherlands; t.k.h.vu@lumc.nl.

Received: April 26, 2024
Accepted: June 26, 2024
Published: July 23, 2024

Citation: Gelmi MC, de Ru AH, van Veelen PA, et al. Protein and mRNA expression in uveal melanoma cell lines are related to GNA and BAP1 mutation status. *Invest Ophthalmol Vis Sci.* 2024;65(8):37. https://doi.org/10.1167/iovs.65.8.37

Purpose. Cell lines are being used in preclinical uveal melanoma (UM) research. Because not all cell lines harbor typical *GNAQ* or *GNA11* hotspot mutations, we aimed at better classifying them and determining whether we could find genetic causes to explain the protein and mRNA expression profiles of the cell lines.

Methods. We studied protein and mRNA expression of 14 UM cell lines and determined the presence of single nucleotide variants and small insertions and deletions with next-generation sequencing and copy number alterations with a single nucleotide polymorphism array. The lists of differentially expressed proteins and genes were merged, and shared lists were created, keeping only terms with concordant mRNA and protein expression. Enrichment analyses were performed on the shared lists.

Results. Cell lines Mel285 and Mel290 are separate from GNA-mutated cell lines and show downregulation of melanosome-related markers. Both lack typical UM mutations but each harbors four putatively deleterious variants in *CTNNB1*, *PPP1R10*, *LIMCH1*, and *APC* in Mel285 and *ARID1A*, *PPP1R10*, *SPG11*, and *RNF43* in Mel290. The upregulated terms in Mel285 and Mel290 did not point to a convincing alternative origin. Mel285 shows loss of chromosomes 1p, 3p, partial 3q, 6, and partial 8p, whereas Mel290 shows loss of 1p and 6. Expression in the other 12 cell lines was related to BAP1 expression.

Conclusions. Although Mel285 and Mel290 have copy number alterations that fit UM, multi-omics analyses show that they belong to a separate group compared to the other analyzed UM cell lines. Therefore, they may not be representative models to test potential therapeutic targets for UM.

Keywords: melanoma, cell lines, mutations

Cell lines are important in preclinical research, as they can be used to study molecular mechanisms and to test new therapies. There are two main types of cell lines: primary cultures and established cell lines. Primary cultures are directly derived from fresh tissue or tumor samples, whereas established cell lines are permanent cultures that continue to proliferate. Primary cultures offer a better representation of tumor heterogeneity, but they have a limited life span and cannot be shared easily with other research groups. In contrast, established cell lines lack heterogeneity and may accumulate or lose mutations over time, but they have an unlimited life span and can be shared by laboratories all over the world.

In uveal melanoma (UM) research, a small number of established primary and metastatic cell lines are available and frequently used in preclinical studies. Most of these cell lines have been studied for typical UM mutations, chromosome abnormalities, expression of melanoma markers, BRCA1-associated protein 1 (BAP1) protein expression, and cell type.[1–4] As the number of available cell lines for this malignancy is limited, many studies use the same set of cell lines.

In the past, some cell lines originally classified as derived from a UM were discovered to have been misidentified.[5] Cell lines OCM-1, OCM-3, and OCM-8 were originally obtained from UM after enucleation, but they were later shown

to carry a *BRAF* mutation, which is typical of cutaneous melanoma.[6–10] These cell lines showed contamination by cutaneous melanoma cell lines M14 and SK-MEL-28.[7–11] Moreover, short tandem repeat (STR) profiling of cell lines OCM-3 and OCM-8 revealed that these two cell lines were not distinct but were derived from the same patient,[5,10] which was also the case for cell lines OCM-1 and MUM2C.[5] These reports of misidentification undermine the validity of studies performed on these cell lines as representing the behavior of UM.

Among the UM cell lines, Mel285 and Mel290 stand out because they do not harbor a mutation in either *GNAQ* or *GNA11*, which are hotspot mutations considered typical for UM.[4,10,12,13] These features may raise several questions, such as whether Mel285 and Mel290 are truly UM cell lines and whether they are representative models to test potential therapeutic targets for UM.

We hypothesized that an analysis of cell line mRNA and protein expression, as well next-generation sequencing (NGS), might tell us more about the origin of the cell lines and would correspond with the different mutation patterns. We therefore analyzed protein and mRNA expression of the Mel285 and Mel290 cell lines and 12 other UM cell lines and analyzed the presence of mutations using NGS and of chromosomal abnormalities with a single nucleotide polymorphism (SNP) array. Due to the uncertainties raised by the mutational status of Mel285 and Mel290 compared to the other UM cell lines, the present study focuses on understanding whether or not the genetic differences are responsible for the different protein and mRNA expression profiles that are observed. We used the mRNA and protein expression data to identify patterns in the data and to test how the 14 different UM cell lines are related.

Methods

Cell Lines

Fourteen UM cell lines were used in this study. Cell line 92.1 was established at the Leiden University Medical Center.[14] Cell line OMM1 was established by G.P.M. Luyten, MD (Erasmus MC, Rotterdam, The Netherlands),[1] and cell lines Mel202, Mel285, Mel290, Mel270, OMM2.5, and OMM2.3 were established by B.R. Ksander, PhD (Schepens Eye Research Institute, Boston, MA, USA).[2,15] These cell lines were cultured in Roswell Park Memorial Institute (RPMI) Medium 1640 Dutch modified media (Life Technologies Europe, Bleiswijk, The Netherlands) supplemented with 10% fetal bovine serum (FBS; PAA Laboratories, Pasching, Austria) and 1% GlutaMAX and 2% penicillin/streptomycin (Life Technologies Europe). Cell lines MP38, MP41, MP46, MP65, MM28, and MM66 were kindly provided by the Curie Institute (Paris, France)[3] and cultured in Iscove's Modified Dulbecco's Medium (IMDM; Life Technologies Europe) containing 20% FBS, 1% GlutaMAX, and 2% penicillin/streptomycin. Cells were incubated in 5% CO_2 at 37°C in monolayers in tissue culture flasks in a humidified incubator. Table 1 summarizes the main features of the cell lines.

Proteomics

For proteomic analysis, all cell lines were cultured in the same medium, to limit variation, and IMDM containing 10% FBS, 1% GlutaMAX, and 2% penicillin/streptomycin was chosen. All cell lines were cultured in triplicate in T75 flasks. When confluency reached 75%, cells were harvested and lysed with a sodium dodecyl sulfate lysis buffer, and proteins were analyzed by tandem mass tag mass spectrometry.

Samples were dissolved in water/formic acid (100/0.1 v/v) and analyzed by online C18 nano high-performance liquid chromatography/tandem mass spectrometry (nano-HPLC MS/MS) with a system consisting of an UltiMate 3000 nano gradient HPLC system (Thermo Fisher Scientific, Bremen, Germany), and an Exploris 480 mass spectrometer (Thermo Fisher Scientific). Fractions were injected onto a cartridge precolumn (300 µm × 5 mm, C18 PepMap, 5 um, 100 A), and eluted via a homemade analytical nano-HPLC column (30 cm × 75 µm, Reprosil-Pur C18-AQ 1.9 µm, 120 A; Dr. Maisch, Ammerbuch, Germany).

Table 1. Summary of the Characteristics of the 14 Uveal Melanoma Cell Lines Used in the Study

Cell Line	Type	GNA11	GNAQ	EIF1AX	SF3B1	BAP1 Mutation	BAP1 Protein	Used for DEA
Mel-285	Primary UM	WT	WT	WT	WT	WT	Pos	Yes
Mel-290	Primary UM	WT	WT	WT	WT	WT	Pos (low)	Yes
92.1	Primary UM	WT	c.626 A>T	c.17 G>A	WT	WT	Pos	Yes
Mel 202	Primary UM	WT	c.626 A>Tc.629 G>A	WT	c.1793 C>T	WT	Pos	Yes
Mel-270	Primary UM	WT	c.626 A>C	WT	WT	WT	Pos	Yes
OMM2.3	Metastatic UM liver; from Mel270	WT	c.626 A>C	WT	WT	WT	Pos	No
OMM2.5	Metastatic UM liver; from Mel270	WT	c.626 A>C	WT	WT	WT	Pos	No
MP38	Primary UM	WT	c.626 A>T	WT	WT	c.68-9_72del	Neg	Yes
MP46	PDX; primary UM	WT	c.626 A>T	WT	WT	Promoter deletion	Neg	Yes
OMM-1	Metastatic UM subcutaneous	c.626 A>T	WT	WT	WT	WT	Pos	Yes
MM28	PDX; metastatic UM liver	c.626 A>T	WT	WT	WT	c.1881 C>A	Neg	Yes
MP41	PDX; primary UM	c.626 A>T	WT	WT	WT	WT	Pos	Yes
MP65	Primary UM	c.626 A>T	WT	WT	WT	c.1717del	Neg	Yes
MM66	PDX; metastatic UM liver	c.626 A>T	WT	WT	WT	WT	Pos	Yes

DEA, differential expression analysis; PDX, patient-derived xenograft.

Investigative Ophthalmology & Visual Science

The gradient was run from 2% to 36% solvent B (20/80/0.1 water/acetonitrile/formic acid v/v) for 120 minutes at 250 nL/min. The nano-HPLC column was drawn to a tip of ~10 µm and acted as the electrospray needle of the MS source. The mass spectrometer was operated in data-dependent MS/MS mode with a cycle time of 3 seconds, with a higher energy collision dissociation (HCD) collision energy at 36% and recording of the MS2 spectrum in the Orbitrap, with a quadrupole isolation width of 1.2 Da. In the master scan (MS1), the resolution was 120,000 and the scan range was 350 to 1600, at an automatic gain control (AGC) target of "standard" at a maximum fill time of 50 ms. A lock mass correction on the background ion m/z = 445.12003 was used. Precursors were dynamically excluded after $n = 1$ with an exclusion duration of 45 seconds and with a precursor range of 30 ppm. Charge states 2 to 5 were included. For MS2 the first mass was set to 110 Da, and the MS2 scan resolution was 45,000 at an AGC target of 200% at a fill time of "auto."

In a post-analysis process, raw data were first converted to peak lists using Proteome Discoverer 2.5 (Thermo Fisher Scientific, Waltham, MA, USA) and then submitted to the UniProt Proteomes • *Homo sapiens* (Human) minimal database (20,205 entries), using Mascot 2.2.07 (www.matrixscience.com) for protein identification. Mascot searches were done with 10-ppm and 0.02-Da deviation for precursor and fragment mass, respectively, and trypsin enzyme was specified. Methionine oxidation and acetyl (protein N-term) were set as a variable modification, and tandem mass tag (on N-term and lysine) and carbamidomethylB were set as static modifications. Peak integration, quantification, and protein ratio determination was carried out using Proteome Discoverer. The mass spectrometry proteomics data have been deposited to the ProteomeXchange Consortium via the PRIDE partner repository[16] with the dataset identifier PXD051055.

Proteome Discoverer was used both for data visualization and differential expression analysis. The $\log_2$ fold change ($\log_2$FC) cut-off was set at 1, and the P value threshold for significance was set at 0.05. Differential expression analyses were performed separately for the comparisons of GNA-wild type versus *GNAQ*-mutated and GNA-wild type versus *GNA11*-mutated cell lines. The lists of differentially expressed proteins were subsequently merged, keeping only the proteins in common.

RNA Sequencing

RNA sequencing (RNAseq) data were acquired from Institut Curie (Paris, France). A panel of 13 UM cell lines (all except OMM2.3) was used for the RNAseq experiment. The isolation of total RNA was done with a NucleoSpin Kit (Macherey-Magel, Düren, Germany). Based on the manufacturer's instructions (Invitrogen, Carlsbad, CA, USA), cDNA synthesis was conducted with MuLV Reverse Transcriptase, under quality assessments by an Agilent 2100 Bioanalyzer (Santa Clara, CA, USA). Libraries were then constructed and sequenced. For the data analysis, reads were mapped against the human reference genome (hg19) using TopHat 2.0.6. Gene expression data were obtained using FeatureCounts from the subread package (v1.5.0). The principal component analysis (PCA) plot was plotted with the R package ggplot2 (R Foundation for Statistical Computing, Vienna, Austria), and heatmaps were plotted with ComplexHeatmap or heatmap.2 (gplot package).

Differential expression analysis was performed with DESeq2, through an in-house shiny app (dgeAnalysis, https://github.com/LUMC/dgeAnalysis). Filtering of low expression genes was performed with a $\log_2$ count per million (CPM) cutoff of 1, and the minimum number of samples meeting the $\log_2$CPM value was set at 25%. The $\log_2$FC cut-off was set at 1, and the false discovery rate (FDR) threshold for significance was set at 0.05. Differential expression analysis was performed separately for the comparisons of GNA-wild type versus *GNAQ*-mutated and GNA-wild type versus *GNA11*-mutated cell lines. The lists of differentially expressed genes were subsequently merged, keeping only the genes in common.

Gene Set Enrichment Analysis

Gene set enrichment analysis (GSEA)[17] was performed with the R package fgsea on a pre-ranked list of genes[18] for the comparisons of GNA-wild type versus *GNAQ*-mutated and GNA-wild type versus *GNA11*-mutated separately. Gene set c8 (cell type signature) from the Molecular Signature Database (MSigDB) was used for the analyses.

Differential Expression and Enrichment Analyses

The lists of down- and upregulated genes were merged with the lists of down- and upregulated proteins, keeping only the shared elements in common. Figure 1 delineates the steps of the differential expression analyses. OMM2.5 and OMM2.3, which are metastatic cell lines derived from the same patient as Mel270, were excluded from the analyses to prevent over-representation of proteins and genes unique to one patient. The shared lists of proteins and genes down-regulated and upregulated in GNA-wild type versus GNA-mutated cell lines were used for enrichment analyses (details are available in Fig. 1).

Enrichment analysis was performed with the Cytoscape plug-in ClueGO, which uses a hypergeometric distribution test and kappa statistics. We focused on Gene Ontology (GO) terms and considered only pathways with $P \leq 0.05$ and used GO term fusion to avoid redundant pathways. P values were corrected with Holm–Bonferroni. GO terms with shared members were grouped, and the name of each group is the name of the most relevant GO term in the group.

STR Profiles

STRs were determined using the AmpFlSTR Identifiler PCR Amplification Plus Kit (Applied Biosystems, Waltham, MA, USA) according to the manufacturer's instructions. DNA was amplified in a Biometra TAdvanced Thermocycler (Westburg Life Sciences, Leusden, The Netherlands), and electrophoresis was performed on the 3730xl DNA Analyzer. Analysis and interpretation of the STR lengths were carried out using GeneMarker 3.0.0 (SoftGenetics, State College, PA, USA) and information outlined in the AmpFlSTR Identifiler Plus Kit User Guide (Table 1).

Copy Number Analysis

Copy number profiles were generated using the Infinium Global Screening Array-24 3.0 BeadChip according to manufacturer's protocols and guidelines (Illumina, San Diego, CA, USA). Normalized output was generated using the Illu-

Investigative Ophthalmology & Visual Science

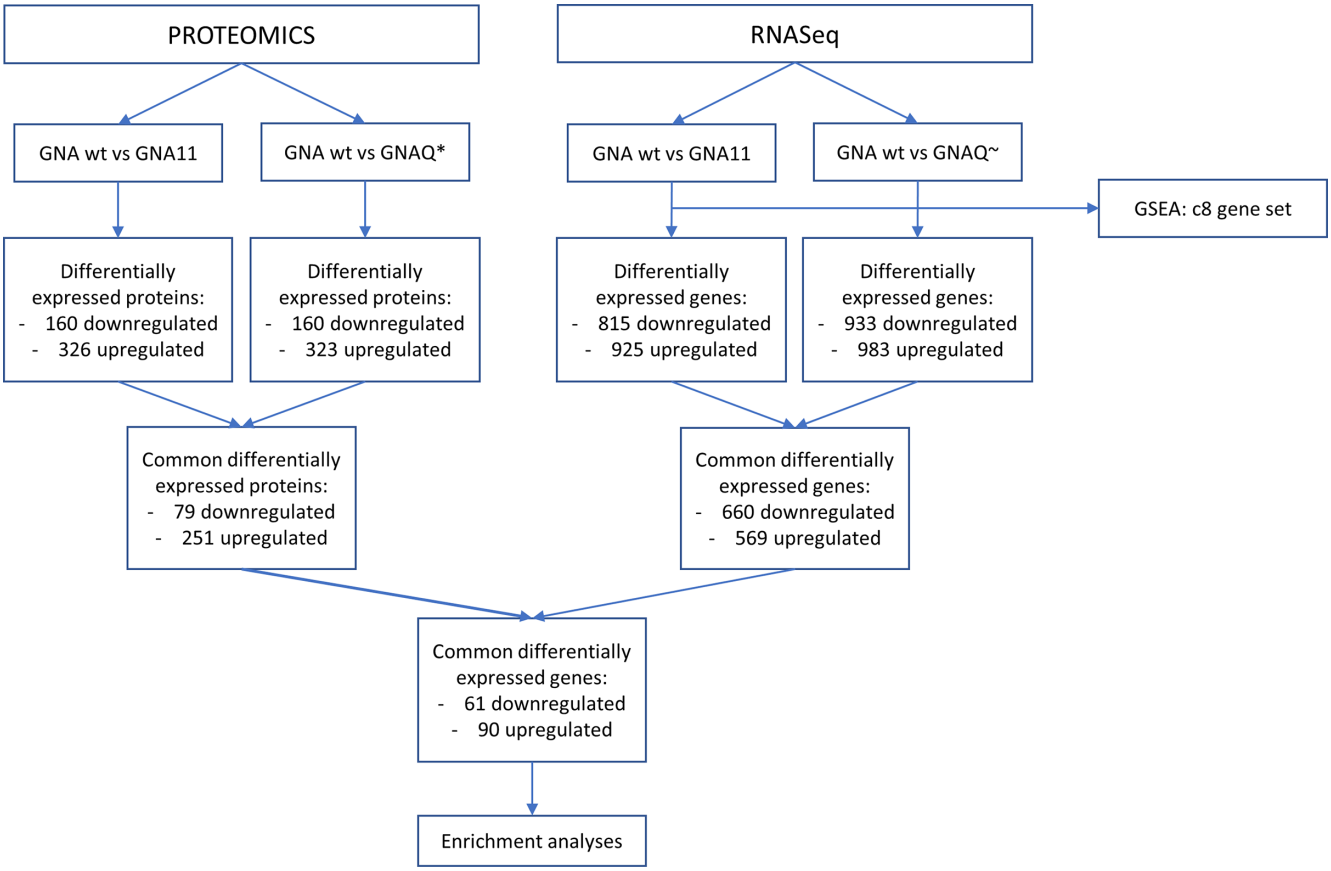

Figure 1. Flowchart showing the steps of the differential expression analysis. Protein expression of GNA-wild type cell lines was compared with protein expression of *GNA11*-mutated and *GNAQ*-mutated cell lines separately, with a logFC threshold of 1 and *P* value cut-off at 0.05. Subsequently, the two lists of differentially expressed proteins were joined, keeping only the proteins that were present on both lists. mRNA expression of GNA-wild type cell lines was compared with mRNA expression of *GNA11*-mutated and *GNAQ*-mutated cell lines separately, with a logFC threshold of 1 and FDR cut-off at 0.05. Subsequently, the two lists of differentially expressed genes were joined, keeping only the genes that were present on both lists. Finally, the lists of differentially expressed proteins and genes were joined, keeping only the terms in common. *Excluding OMM2.3 and OMM2.5. ~Excluding OMM2.5.

mina GenomeStudio Genotyping Module 2.0.5 and imported into Nexus Copy Number 10.0 (Biodiscovery, Hawthorne, CA, USA), processed with the Nexus BioDiscovery FASST2 segmentation algorithm, and visually inspected.

NGS Analyses

The presence of single nucleotide variants (SNVs) and small insertions and deletions (InDels) was investigated with targeted NGS. The Ion PGM Torrent Server (Thermo Fisher Scientific) was used according to the manufacturer's protocol, and hg19 was used as reference genome. Intronic and synonymous variants were excluded from the analysis. Potentially relevant variants were selected if they were predicted to be protein altering and if they were rare. When multiple transcripts were reported for one gene, the transcript labeled as "MANE Select" in the National Center for Biotechnology Information (NCBI) database was considered. The MANE (Matched Annotation from NCBI and EMBL-EBI) project combines information from Refseq transcripts and Ensembl/GENCODE and identifies as "MANE Select" one transcript at each protein-coding locus that is representative of the biology at that locus.[19] We used Mutalisk[20] and Sigprofiler[21] assignment to determine if a sunlight exposure signal was present in Mel285 and Mel290. Additionally, we determined if we could find (likely) pathogenic variants[22] in frequently affected melanoma genes, including cutaneous, acral, and uveal melanoma.

Results

We collected a set of 14 UM cell lines, all of which have been published and used in experimental studies.[1–3,14,15] Of the 14 cell lines, nine were derived from primary UM and five from metastases (Table 1). The majority of primary UM are known to carry a mutation activating the Gα-q pathway, including mutations in *GNAQ*, *GNA11*, *CYSLTR2*, or *PLCB4*. According to the literature, five of the assumed UM cell lines have a mutation in *GNA11* and seven in *GNAQ*.[3,4,10] As already known, two of the cell lines in our panel, Mel285 and Mel290, lack a mutation in *GNAQ* or *GNA11*. One cell line (92.1) has an *EIF1AX* mutation, one (Mel202) a mutation in *SF3B1*, and three a mutation in the *BAP1* gene. One cell line (MP46) does not express *BAP1*, but a deletion in its promoter region has recently been identified.[23] In order to determine whether cell lines matched the ones on which we previously reported, STR profiles were performed.

Investigative Ophthalmology & Visual Science

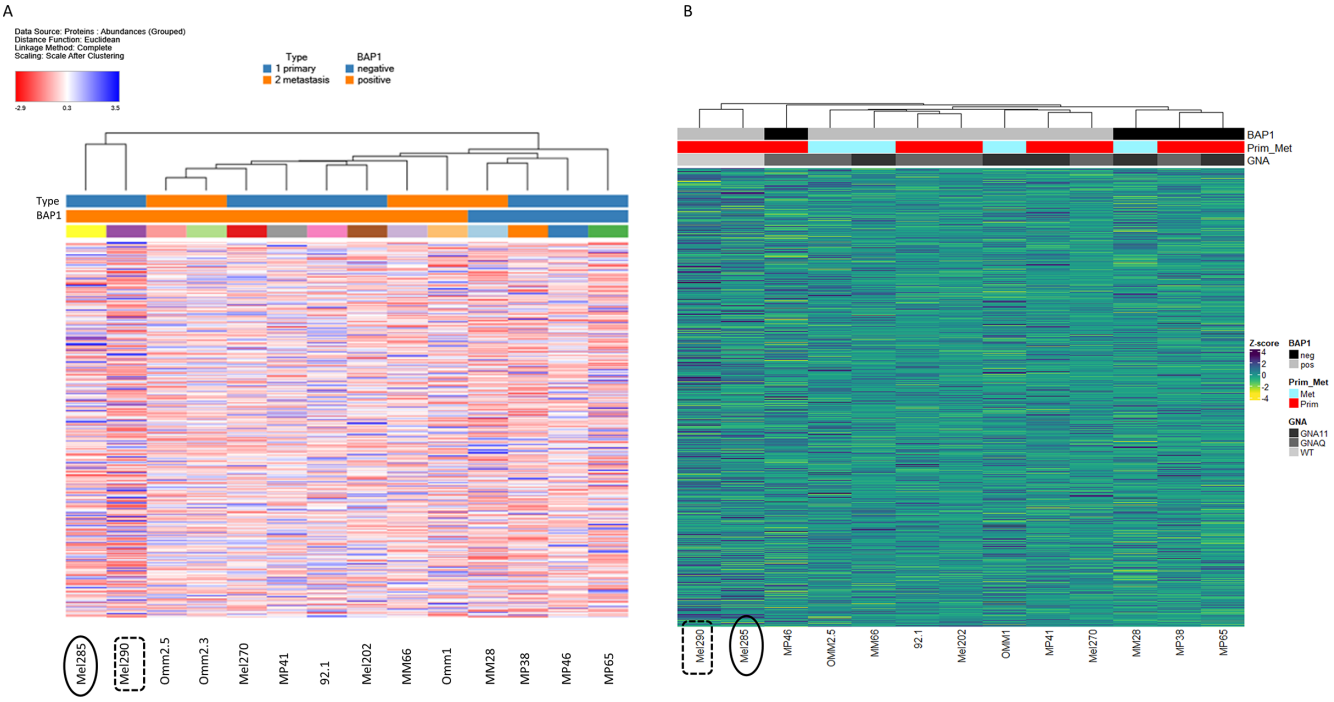

Figure 2. Heatmap showing the expression of all the proteins (**A**) and genes (**B**) across all cell lines. The dendrogram shows that Mel285 (*oval*) and Mel290 (*dashed rectangle*) cluster separately from the other cell lines. Part (**A**) was plotted with Proteome Discoverer, and part (**B**) was plotted with the ComplexHeatmap package in R.

STR Profiles

The STR profiles of all 14 cell lines were compared to the results described in the Cellosaurus release 46 database (Swiss Institute of Bioinformatics, Lausanne, Switzerland)[24] and were also compared with the profiles previously reported in the literature.[3,4] The STR of Mel290 matched the previous profile in all 16 loci, and the STR of Mel285 shared similarity at 15/16 loci (D3S1358 was originally 15;17 and is now 15;15). However, the current profile of Mel285 did fully match the STR profile performed in 2016 by BaseClear BV (Leiden, The Netherlands) for our institution. The STR profiles of cell lines Mel270, Omm2.3, Omm2.5, 92.1, MM28, MP38, and MP46 matched the previous profiles in all 16 loci, whereas cell lines Mel202, Omm1, MP41, and MP65 showed a mismatch in one allele of one locus, and MM66 showed discrepancies in one allele of two loci. Careful inspection of the profiles showed that the discrepancies in Mel202 and Omm1 were due to slight differences in interpretation of the peaks. Moreover, the discrepancies in cell lines Mel202 and Omm1 matched the STR profiles reported in the Cellosaurus and by Griewank et al.[10] and Amirouchene-Angelozzi et al.,[3] whereas the discrepancies in cell lines MP65 and MM66 matched STR profiles performed in our institution in 2020. Hence, we can assume that the identity of these cell lines has been confirmed, although some may have slightly deviated from the original.

Protein and RNA Expression

In order to compare expression profiles between the cell lines, we analyzed the proteomic and mRNA content of the 14 cell lines and performed unsupervised cluster analyses. Based on the protein and mRNA expression heatmaps, Mel285 and Mel290 formed their own clusters in both dendrograms (Figs. 2A, 2B). In the proteomic analysis, the four cell lines that did not express BAP1 clustered separately from the 10 with BAP1 expression. In the RNAseq expression analysis, three of the four BAP1-negative cell lines clustered together, separate from the others.

Each proteome analysis was performed on material obtained from three separate culture flasks for each cell line. The triplicate results for each of the 14 cell lines are shown in the PCA plot in Figure 3A, and the PCA plot in Figure 3B is derived from RNAseq data (one dot per cell line). Cell lines Mel285 and Mel290 clustered separately from all other UM cell lines, along the principal component with the highest variation (34% in proteomics, 45% in RNAseq) (Fig. 3). In both PCA plots, the GNA-mutated cell lines separated into the BAP1-positive and -negative cell lines. From these analyses, we can conclude that the main source of variation in our panel of UM cell line is the presence of a *GNAQ* or *GNA11* mutation and the second source of variation is BAP1 expression.

Differentially Expressed RNA and Proteins

The unsupervised cluster analyses show a clear difference between cell lines Mel285 and Mel290 versus the other cell lines. We wondered whether specific pathways would differ between the two GNA-wild type and GNA-mutated cell lines. For the RNAseq analyses, we set the $\log_2$FC threshold at 1 and the FDR threshold for significance at 0.05, and for the proteomics analysis we set the $\log_2$FC threshold at 1 and the *P* value threshold for significance at 0.05. Mel285 and Mel290 had 61 downregulated and 90 upregulated genes and proteins compared to GNA-mutated cell lines (Fig. 1).

Investigative Ophthalmology & Visual Science

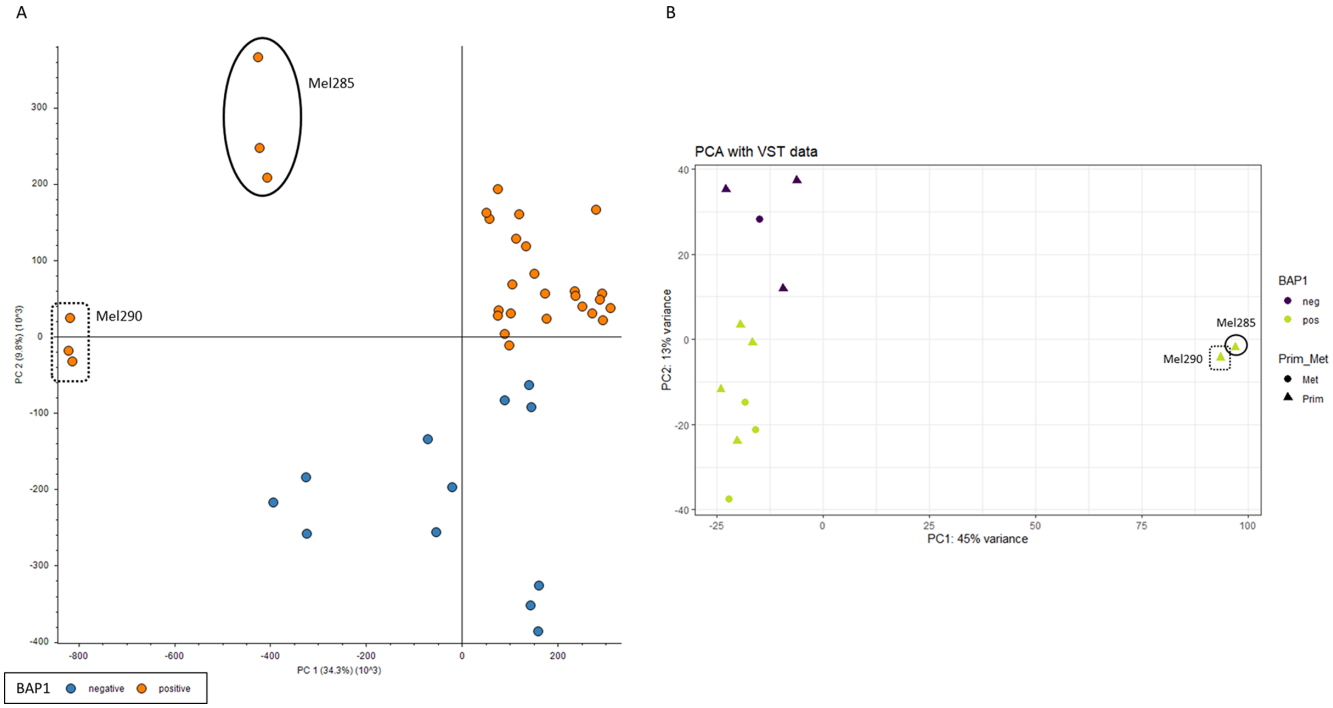

Figure 3. PCA plots showing distances between cell lines. (**A**) PCA plot created with Proteome Discoverer using normalized protein abundance data (each cell line is plotted in triplicate). *Blue* indicates BAP1-negative, and *orange* indicates BAP1-positive. (**B**) PCA plot created with ggplot2 package in R using variance stabilizing transformation (VST)-transformed RNAseq data. *Circles* indicate metastatic cell lines; *triangles* indicate primary cell lines; *purple* indicates BAP1-negative; and *green* indicates BAP1-positive.

Most Downregulated Genes and Proteins Relate to Pigmentation

In order to obtain the major differences between cell lines, we performed enrichment analysis of differentially expressed genes and proteins with the ClueGO app in Cytoscape. The protein and the mRNA expression data demonstrate that gene sets related to melanosomes are clearly overrepresented among the downregulated GO terms, along with gene sets related to oxidoreductase activity (Fig. 4). We therefore focused on the pigment and melanocyte-related markers and evaluated their mRNA and protein expression. As the heatmaps in Figure 5 and Supplementary Table S1 show, most of the melanocyte markers are lower in Mel285 and Mel290 compared to the GNA-mutated cell lines. The dendrograms of the heatmaps clearly show that Mel285 and Mel290 cluster separately when considering pigment-related genes and proteins (Fig. 5).

Single Nucleotide Variants

The clear separation between GNA-wild type and GNA-mutated cell lines and the downregulation of melanocyte and pigment pathways in GNA-wild type cell lines are in agreement with previous mutation analyses[10] and may call into question the identity of Mel285 and Mel290 as truly UM cell lines. Therefore, we determined the presence of SNVs and small InDels by NGS. NGS showed that Mel285 and Mel290 not only lack *GNAQ* and *GNA11* mutations but also do not carry any of the other typical UM mutations either, including those in *CYSLTR2*, *PLCB4*, *EIF1AX*, and *SF3B1*. We did not find alternative splicing mutations in *SRSF2* reported in other publications.[25,26] After selecting the variants by protein-altering ability and rarity, we identified four SNVs in Mel285 and four SNVs in Mel290. Table 2 shows details of the SNVs found in Mel285 and Mel290.

Mel285 carries the following putative deleterious SNVs: *CTNNB1* c.A32G:p.D11G, *PPP1R10* c.T1583C:p.M528T (also present in Mel290), *LIMCH1* c.2418_2419del:p.E810Afs*3, and *APC* c.A4249C:p.I1417L. The SNVs in *CTNNB1* and *PPP1R10* have not been reported before, whereas the SNVs in *APC* and *LIMCH1* have been reported before, but not in UM. The SNV in *APC* is classified as of uncertain significance, whereas the *LIMCH1* variant has been reported in the COSMIC database (COSV58272067/COSM253016) and has been found in some samples of carcinoma of the endometrium, large intestine, stomach, breast, and ovary.

Mel290 has the following SNVs: *ARID1A* c.C862G:p.Q288E, *PPP1R10* c.T1583C:p.M528T (also present in Mel285), *SPG11* c.1347_1348TG:p.I450V, and *RNF43* c.G776T:p.W259L. The SNVs in *ARID1A*, *PPP1R10*, and *RNF43* have not been reported before, whereas the SNV in *SPG11* has been reported and classified as a missense variant. These results do not suggest a specific non-UM cell origin or potential mix-up by another known cancer cell line.

Mel285 and Mel290 Do Not Have an Ultraviolet Signature

Ultraviolet (UV) light induces a characteristic pattern of elevated C to T transitions at dipyrimidine sites.[27] Both familial and sporadic melanoma have genes that are typically impacted by somatic mutations.[28,29] Mutagens, including sunlight exposure, can result in elevated levels of charac-

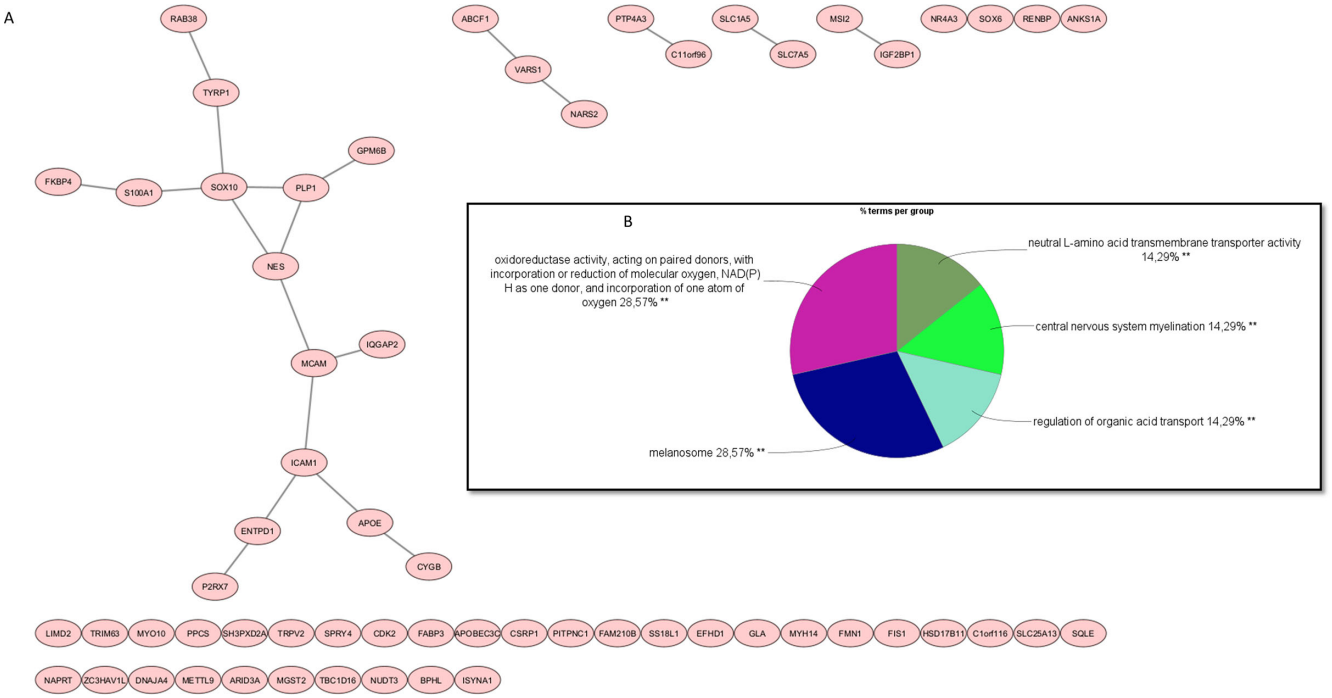

Figure 4. Proteins and genes downregulated in cell lines Mel285 and Mel290 are enriched in melanosome and pigment-related pathways. (**A**) STRING network showing the genes and proteins downregulated in GNA-wild type cell lines Mel285 and Mel90, obtained from the shared list of differentially expressed terms from proteomics and RNAseq data. Computed with Cytoscape. (**B**) Pie chart showing the distribution of GO term groups downregulated in GNA-wild type versus GNA-mutated cell lines, calculated with the ClueGO app in Cytoscape on the list of downregulated genes and proteins, with GO term fusion.

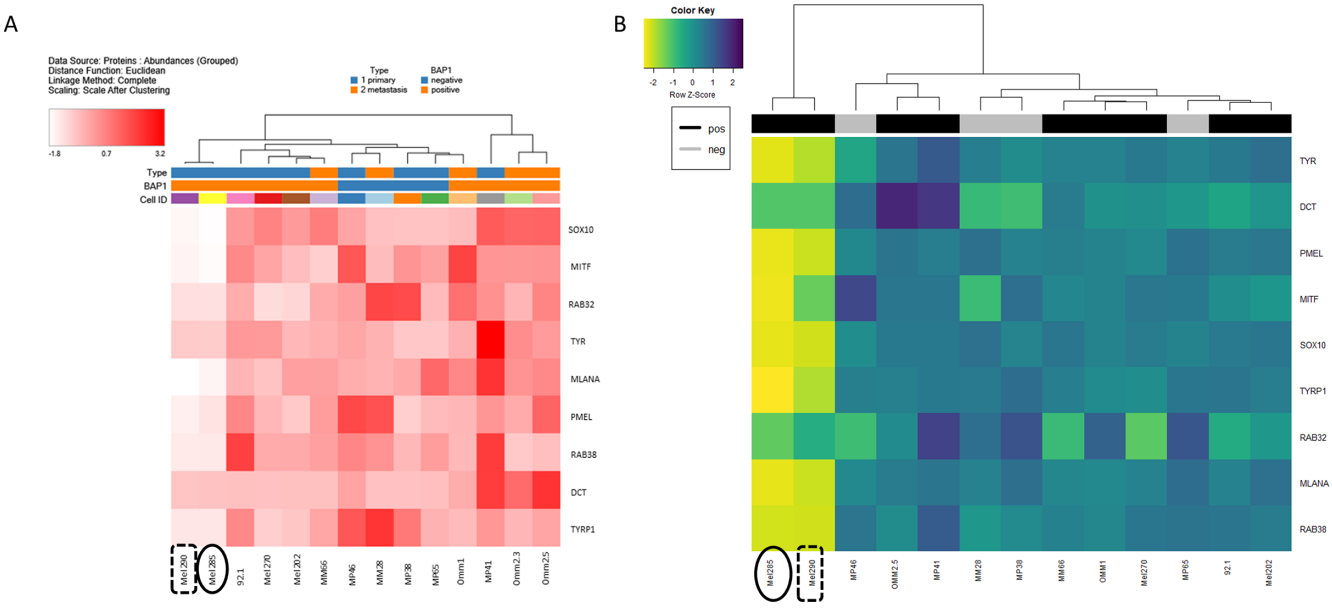

Figure 5. Pigment-related proteins and genes are downregulated in GNA-wild type cell lines Mel285 (oval) and Mel290 (dashed rectangle). (**A**) Heatmap showing the expression of pigment-related proteins (grouped protein abundance, with one value per cell line). Euclidean distances, scaled after clustering, were plotted with Proteome Discoverer. (**B**) Heatmap showing expression of pigment-related genes (VST-transformed RNAseq data). Euclidean distances, scaled after clustering, were plotted with the heatmap.2 function in R.

teristic patterns of mutations, including mutation signatures, with signatures SBS7a to SBS7d being typical for UV light exposure.[30] Somatic mutations are determined by comparing germline DNA to tumor DNA. The remaining mutations, often non-heterozygous and with a low frequency in population frequency databases, can be used to determine the tumor mutation signature. We studied cell lines Mel285 and Mel290 to determine if a sunlight exposure signal was

Investigative Ophthalmology & Visual Science

Table 2. Overview of SNVs Detected With NGS (Ion PGM Torrent Server)

Cell Line	Gene	Location	Transcript	Variant	Reported
Mel285	*CTNNB1*	3p22.1	NM_001904	c.A32G:p.D11G	—
	PPP1R10	6p21.33	NM_002714	c.T1583C:p.M528T	—
	LIMCH1	4p13	NM_001330672	c.2418_2419del:p.E810Afs*3	COSV58272067/COSM253016
	APC	5q22.2	NM_000038	c.A4249C:p.I1417L	rs200166878 (uncertain significance)
Mel290	*ARID1A*	11p36.11	NM_006015	c.C862G:p.Q288E	—
	PPP1R10	6p21.33	NM_002714	c.T1583C:p.M528T	—
	SPG11	15q21.1	NM_025137	c.1347_1348TG:p.I450V	rs796921512 (missense variant)
	RNF43	17q22	NM_017763	c.G776T:p.W259L	—

The variants were selected if they were putatively deleterious and rare.

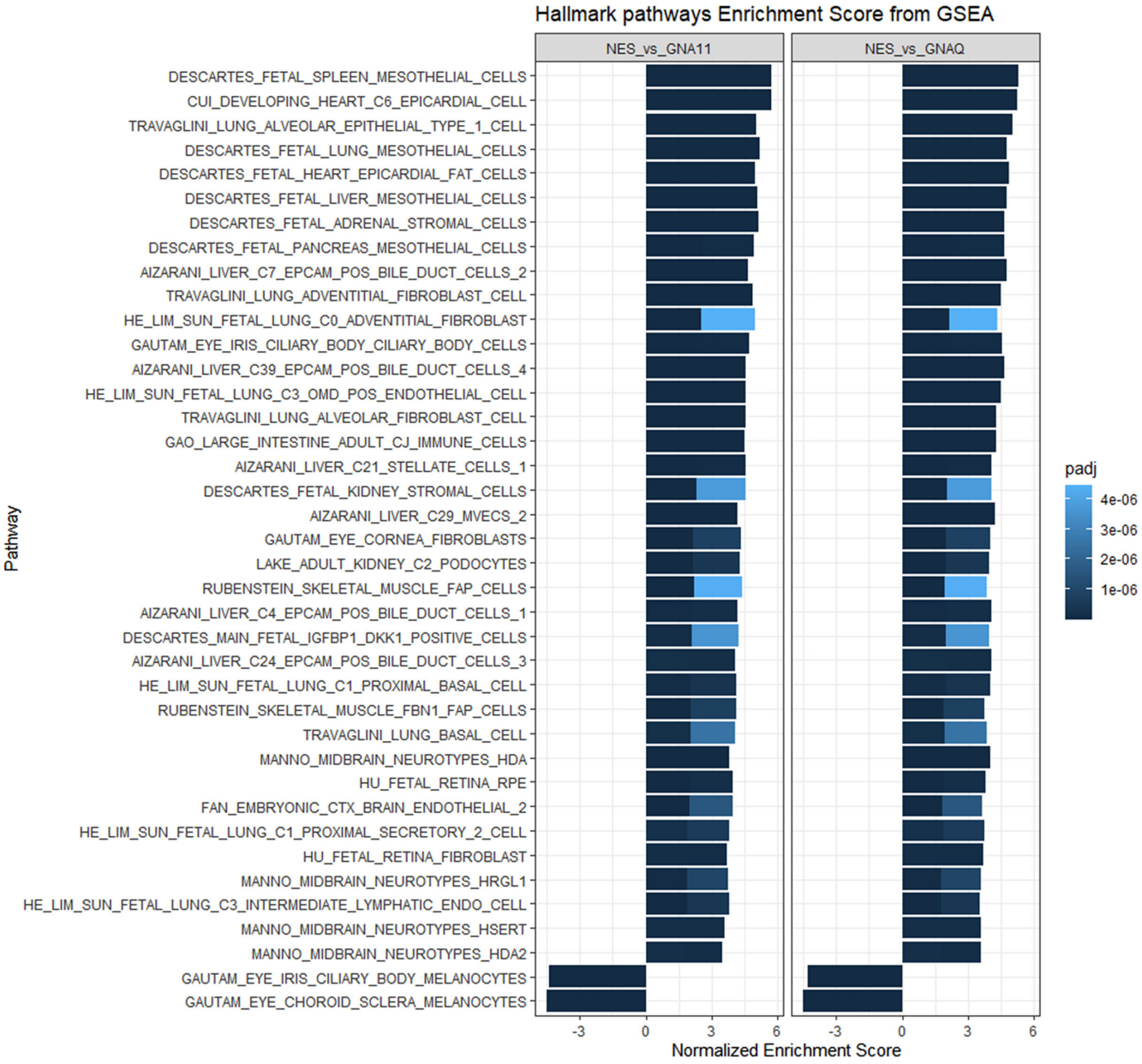

Figure 6. GSEA comparing cell type signature gene sets (c8), using mRNA expression data. GNA-wild type cell lines Mel2S85 and Mel290 were compared to *GNAQ*-mutated cell lines and to *GNA11*-mutated cell lines separately. The bar plot shows the top 50 differentially enriched gene sets.

Investigative Ophthalmology & Visual Science

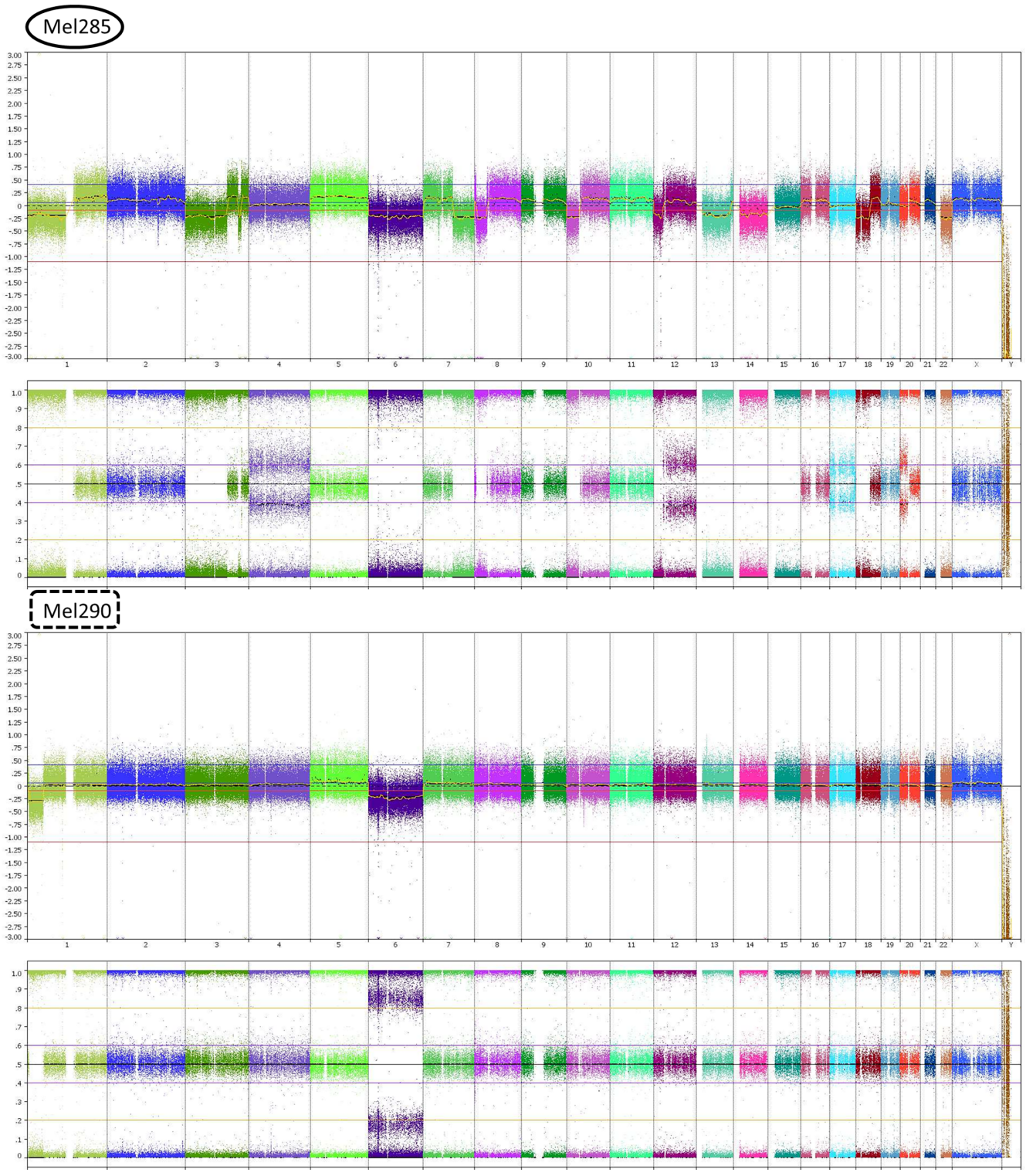

Figure 7. Chromosomal alterations tested by SNP array of cell lines Mel285 (*oval*) and Mel290 (*dashed rectangle*).

present and if we could find (likely) pathogenic variants[22] in frequently affected melanoma genes, including cutaneous, acral and uveal melanoma. Interestingly, we could not identify (likely) pathogenic changes in uveal melanoma or other melanoma-related genes; the mutation signature of both cell lines mostly resembled SBS5 rather than SBS7a to SBS7d. This is indicative of mechanisms different from UV light responsible for tumor formation, although using a single sample, cultured cell lines, and a targeted gene panel to determine mutation signatures might not give robust results.

Most Upregulated Pathways Are Heterogeneous

In order to shed more light on the identity of Mel285 and Mel290, we focused on the pathways that are upregulated in Mel285 and Mel290 versus GNA-mutated cell lines, based

Investigative Ophthalmology & Visual Science

on the shared list of upregulated genes and proteins. The pie chart in Supplementary Figure S1 shows that the most upregulated pathways in Mel285 and Mel290 are related to "formation of primary germ layer," "negative regulation of T cell receptor signaling pathways," "regulation of wound healing," "focal adhesion assembly," "cell–cell contact zone," and "negative regulation of p38MAPK cascade." The heterogeneity of upregulated pathways does not allow us to confidently point to any other cell type as a potential origin.

Gene Set Enrichment Analysis

Next, we used the mRNA expression data to perform GSEA with cell type signature gene sets (c8), which contain markers for specific cell types identified in single-cell sequencing studies. We performed this analysis to compare GNA-wild type versus *GNAQ*-mutated and GNA-wild type versus *GNA11*-mutated separately. As shown in Figure 6, the two most downregulated gene sets were GAUTAM_IRIS_CILIARY_BODY_MELANOCYTES and GAUMAT_CHOROID_SCLERA_MELANOCYTES, which further justifies potential doubts about the identity of Mel285 and Mel290. However, gene sets positively enriched in Mel285 and Mel290 versus GNA-mutated cell lines were related to many different cell types. Hence, it is difficult to confidently classify these cell lines as coming from a specific alternative source.

Chromosome Aberrations Give a Mixed Picture

The SNP array in Figure 7 shows that the two cell lines have very different chromosome alterations. The SNP array of Mel285 shows several chromosome alterations across the whole genome and indicate that it may be polyploid, possibly with four copies of each chromosome as the baseline. Some of the copy number variations in Mel285 are frequently seen in UM: loss of 1p, loss of 3p, partial loss of 3q, loss of 6q, and partial loss of 8p. However, the array additionally shows a small gain in 3q, loss of 6p, and loss in many other chromosomes, as well as no gain in chromosome 8q. Mel290 shows loss of 1p and of the whole chromosome 6, with no alterations in chromosome 3 or 8. Because one group reported the presence of 8q24.1–8q24.2 gain in Mel290,[31] we specifically investigated this area, but we did not find any copy number alteration (Supplementary Fig. S2).

Discussion

UM is characterized by specific mutations in the genes that code for G proteins or G protein targets, such as in *GNAQ*, *GNA11*, *CYSLTR2*, or *PLCB4*, as well as secondary mutations in *EIF1AX*, *SF3B1*, and *BAP1*. Mel285 and Mel290 are two UM cell lines that are being extensively used to study the processes behind UM and to test potential therapies. However, as has been pointed out in previous publications, these two cell lines do not carry a *GNAQ* or a *GNA11* mutation and do not express melanocyte markers.[4,10,32] In addition, we did not find one of the other characteristic primary or secondary mutations, either. Differential expression analyses with proteomics and RNAseq data showed that melanocyte markers and melanosome-related pathways were significantly downregulated in Mel285 and Mel290 compared to GNA-mutated cell lines (Figs. 4, 5). A potential connection between the lack of melanocyte markers and the lack of a *GNAQ* or *GNA11* mutation can be hypothesized, based on the results of a study in mice by van Raamsdonk et al.,[33] who showed that mutations in *GNAQ* and *GNA11* caused a phenotype with increased dermal pigmentation and that knock out of *GNAQ* and *GNA11* reversed this effect. A different theory was brought forward by van Dinten et al.,[32] who analyzed both UM and cutaneous melanoma cell lines and reported a difference in methylation of the NruI regulator site of the Melan-A promoter between Melan-A–positive and Melan-A–negative cell lines. However, if we combine the results of the differential expression and mutation analyses with the fact that Mel285 and Mel290 clearly cluster separately from the GNA-mutated cell lines, both with protein and mRNA expression data (Figs. 2, 3), we may call into question the identity of these two cell lines as truly UM cell lines. For this reason, we focused on a comparison of proteins, genes and pathways. As evident from Supplementary Figure S1 and Figure 6, these analyses produced a heterogeneous picture characterized by myriad very different pathways and gene sets upregulated in Mel285 and Mel290 compared to the other 12 UM cell lines, which does not clearly point toward a convincing alternative origin for these cell lines. We may also hypothesize that the reason behind this heterogeneity is that Mel285 and Mel290 are very different from each other, because they are derived from two different tumors in two different patients.[4] We could therefore postulate that the only real element in common is the fact that they are both different from other UM cell lines, causing them to cluster together in the analyses presented in Figures 2 and 3. If that is the case, we can imagine that the differences between Mel285 and Mel290 may be the reason why they did not show a clear-cut gene expression signature when considered together.

Mutation analysis of Mel285 and Mel290 by NGS identified four variants in each cell line, with one variant detected in both cell lines. Only one variant present in Mel285 has previously been reported in tumor samples (*LIMCH1* c.2418_2419del:p.E810Afs*3) (Table 2). Of the seven genes, some are of more interest than others. *CTNNB1* and *APC* are involved in the Wnt pathway; when the Wnt pathway is activated, *CTNBB1* translocates into the nucleus and activates Wnt response genes, whereas *APC* is part of a complex that ubiquitinates and targets *CTNNB1* for proteasome degradation.[34] Both *CTNNB1* and *APC* are involved in several types of cancer, with opposing roles. The most notable association is with colorectal cancer, but the reported variants are different from the SNVs we found in our cell lines.[35–39]

PPP1R10 encodes a protein called PNUTS, which regulates protein phosphatase 1; promotes tumorigenesis in cancer cell lines, possibly through interaction with phosphatase and tensin homolog (PTEN) or Myc; and is correlated with negative prognosis in prostate cancer.[40–42] LIMCH1 is involved in the regulation of cell motility, and its downregulation has been linked to increased cell migration in HeLa cells and to poorer prognosis in lung cancer.[43–45] ARID1A is part of the SWItch/Sucrose Non-Fermentable (SWI/SNF) family of proteins and is mutated in several cancer types.[46,47] *ARID1A* mutations have been reported in some cutaneous melanoma cases and have been linked to a UV signature.[48,49] RNF43 is both a target and a negative regulator of the Wnt receptor Frizzled.[50–52] Mutations in *RNF43* are present in endometrial, gastric and colorectal cancer,[53,54] and, in colorectal cancer, *RNF43* mutations are associated with microsatellite instability.[55–57] Finally, *SPG11* has never

Investigative Ophthalmology & Visual Science

been associated with cancer, but mutations are common in recessive hereditary spastic paraplegia.[58–61]

One element that weighs in favor of Mel285 and Mel290 being considered UM cell lines is their chromosome status (Fig. 7): The loss of 1p and loss of 6q are present in both Mel285 and Mel290, and Mel285 also shows a loss of 3p and partial loss of 3q. Mel285 is likely polyploid, given the discrepancies between the expected and observed allelic frequency plots and logR ratios. Gain of 8q has been reported previously in Mel285 (three or four copies, depending on the sources) but it is not present in this study.[4,62] Mel290 showed disomy in chromosome 8q in our analysis and in most studies present in the literature.[4] Only one study reported a gain in 8q24.1–8q24.2 in Mel290,[31] but this was not present in our data. This could be due to a real absence of the alteration or the presence of the alteration in a very small proportion of cells, thus falling below the limit of detection. Even though some typical UM chromosome aberrations are present, the entire chromosome 6 is lost in both cell lines, which is not typical of UM, and Mel285 shows many additional alterations.

The other UM cell lines for which we analyzed the protein and RNAseq expression clustered according to their BAP1 expression. Four cell lines that lacked BAP1 expression clustered separately from the other four cell lines when we looked at protein expression, and three of these four did so for mRNA expression. One of these four, MP46, which lacks the BAP1 protein due to a deletion in its regulatory sequences, clustered separately from the other three BAP1-negative cell lines in the RNAseq analyses. The variability in genetic backgrounds of the available cell lines will allow them to be used as fine models for testing new drugs. However, authors who report on tests with these cell lines should always indicate where their cell lines come from and check their identity to prevent accidental mistakes in cell line identification.

At this stage, we cannot confidently confirm or deny the identity of Mel285 and Mel290 as UM cell lines, but we can state that these two cell lines belong to a separate group than GNA-mutated cell lines and, therefore, may not be representative models for the study of potential therapeutic targets for UM. In general, researchers should be extremely careful when deciding to use cell lines with atypical features, such as Mel285 and Mel290, as they may not be representative of the condition they are studying. What also is evident from our data is that, in addition to the presence of a *GNAQ* or *GNA11* mutation, BAP1 expression influences the protein and mRNA expression in these UM cell lines.

Acknowledgments

The authors thank Aart G. Jochemsen, PhD (Department of Cell and Chemical Biology, Leiden University Medical Center) and Peter de Knijff, PhD (Department of Human Genetics, Leiden University Medical Center) for sharing the STR profiles performed on UM cell lines in 2020. The authors also thank Leon Mei, PhD, for help with the dgeAnalysis app.

MCG supported by the Bontius Foundation, Oogfonds, the Sam Fund, the Leiden University Fund, P.A. Jager-van Gelder Fund, the Blinden-Penning Foundation, and Associazione Scientifica Retinoblastoma ed Oncologia Oculare.

Disclosure: **M.C. Gelmi**, None; **A.H. de Ru**, None; **P.A. van Veelen**, None; **R.T.N. Tjokrodirijo**, None; **M.-H. Stern**, None; **A. Houy**, None; **R.M. Verdijk**, None; **T.H.K. Vu**, None; **B.R. Ksander**, None; **J. Vaarwater**, None; **E. Kilic**, None; **E. Brosens**, None; **M.J. Jager**, None

References

1. Luyten GP, Naus NC, Mooy CM, et al. Establishment and characterization of primary and metastatic uveal melanoma cell lines. *Int J Cancer*. 1996;66:380–387.
2. Chen PW, Murray TG, Uno T, Salgaller ML, Reddy R, Ksander BR. Expression of MAGE genes in ocular melanoma during progression from primary to metastatic disease. *Clin Exp Metastasis*. 1997;15:509–518.
3. Amirouchene-Angelozzi N, Nemati F, Gentien D, et al. Establishment of novel cell lines recapitulating the genetic landscape of uveal melanoma and preclinical validation of mTOR as a therapeutic target. *Mol Oncol*. 2014;8:1508–1520.
4. Jager MJ, Magner JA, Ksander BR, Dubovy SR. Uveal melanoma cell lines: where do they come from? (An American Ophthalmological Society Thesis). *Trans Am Ophthalmol Soc*. 2016;114:T5.
5. Folberg R, Kadkol SS, Frenkel S, et al. Authenticating cell lines in ophthalmic research laboratories. *Invest Ophthalmol Vis Sci*. 2008;49:4697–4701.
6. Kan-Mitchell J, Mitchell MS, Rao N, Liggett PE. Characterization of uveal melanoma cell lines that grow as xenografts in rabbit eyes. *Invest Ophthalmol Vis Sci*. 1989;30:829–834.
7. Calipel A, Lefevre G, Pouponnot C, Mouriaux F, Eychene A, Mascarelli F. Mutation of B-Raf in human choroidal melanoma cells mediates cell proliferation and transformation through the MEK/ERK pathway. *J Biol Chem*. 2003;278:42409–42418.
8. Kilic E, Bruggenwirth HT, Verbiest MM, et al. The RAS-BRAF kinase pathway is not involved in uveal melanoma. *Melanoma Res*. 2004;14:203–205.
9. Maat W, Kilic E, Luyten GP, et al. Pyrophosphorolysis detects B-RAF mutations in primary uveal melanoma. *Invest Ophthalmol Vis Sci*. 2008;49:23–27.
10. Griewank KG, Yu X, Khalili J, et al. Genetic and molecular characterization of uveal melanoma cell lines. *Pigment Cell Melanoma Res*. 2012;25:182–187.
11. Korch C, Hall EM, Dirks WG, et al. Authentication of M14 melanoma cell line proves misidentification of MDA-MB-435 breast cancer cell line. *Int J Cancer*. 2018;142:561–572.
12. Van Raamsdonk CD, Bezrookove V, Green G, et al. Frequent somatic mutations of GNAQ in uveal melanoma and blue naevi. *Nature*. 2009;457:599–602.
13. Van Raamsdonk CD, Griewank KG, Crosby MB, et al. Mutations in *GNA11* in uveal melanoma. *N Engl J Med*. 2010;363:2191–2199.
14. De Waard-Siebinga I, Blom DJ, Griffioen M, et al. Establishment and characterization of an uveal-melanoma cell line. *Int J Cancer*. 1995;62:155–161.
15. Verbik DJ, Murray TG, Tran JM, Ksander BR. Melanomas that develop within the eye inhibit lymphocyte proliferation. *Int J Cancer*. 1997;73:470–478.
16. Perez-Riverol Y, Bai J, Bandla C, et al. The PRIDE database resources in 2022: a hub for mass spectrometry-based proteomics evidences. *Nucleic Acids Res*. 2022;50:D543–D552.
17. Subramanian A, Tamayo P, Mootha VK, et al. Gene set enrichment analysis: a knowledge-based approach for interpreting genome-wide expression profiles. *Proc Natl Acad Sci USA*. 2005;102:15545–15550.
18. Korotkevich G, Sukhov V, Budin N, Shpak B, Artyomov MN, Sergushichev A. An algorithm for fast preranked gene set

enrichment analysis using cumulative statistic calculation. *bioRxiv*, https://doi.org/10.1101/060012.
19. Morales J, Pujar S, Loveland JE, et al. A joint NCBI and EMBL-EBI transcript set for clinical genomics and research. *Nature*. 2022;604:310–315.
20. Lee J, Lee AJ, Lee JK, et al. Mutalisk: a web-based somatic MUTation AnaLyIS toolKit for genomic, transcriptional and epigenomic signatures. *Nucleic Acids Res*. 2018;46:W102–W108.
21. Diaz-Gay M, Vangara R, Barnes M, et al. Assigning mutational signatures to individual samples and individual somatic mutations with SigProfilerAssignment. *Bioinformatics*. 2023;39:btad756.
22. Richards S, Aziz N, Bale S, et al. Standards and guidelines for the interpretation of sequence variants: a joint consensus recommendation of the American College of Medical Genetics and Genomics and the Association for Molecular Pathology. *Genet Med*. 2015;17:405–424.
23. Gentien D, Saberi-Ansari E, Servant N, et al. Multi-omics comparison of malignant and normal uveal melanocytes reveals molecular features of uveal melanoma. *Cell Rep*. 2023;42:113132.
24. Bairoch A. The Cellosaurus, a cell-line knowledge resource. *J Biomol Tech*. 2018;29:25–38.
25. Robertson AG, Shih J, Yau C, et al. Integrative analysis identifies four molecular and clinical subsets in uveal melanoma. *Cancer Cell*. 2017;32:204–220.e15.
26. van Poppelen NM, Drabarek W, Smit KN, et al. *SRSF2* mutations in uveal melanoma: a preference for in-frame deletions? *Cancers (Basel)*. 2019;11:1200.
27. Brash DE. UV signature mutations. *Photochem Photobiol*. 2015;91:15–26.
28. Cancer Genome Atlas Network. Genomic classification of cutaneous melanoma. *Cell*. 2015;161:1681–1696.
29. Hayward NK, Wilmott JS, Waddell N, et al. Whole-genome landscapes of major melanoma subtypes. *Nature*. 2017;545:175–180.
30. Alexandrov LB, Kim J, Haradhvala NJ, et al. The repertoire of mutational signatures in human cancer. *Nature*. 2020;578:94–101.
31. Director-Myska AE, White JS, McLean IW. Molecular cytogenetic characterization of ten uveal melanoma cell lines. In: Jager MJ, Niederkorn JY, Ksander BR, eds. *Uveal Melanoma: A Model for Exploring Fundamental Cancer Biology*. Boca Raton, FL: CRC Press; 2004:89–114.
32. van Dinten LC, Pul N, van Nieuwpoort AF, Out CJ, Jager MJ, van den Elsen PJ. Uveal and cutaneous melanoma: shared expression characteristics of melanoma-associated antigens. *Invest Ophthalmol Vis Sci*. 2005;46:24–30.
33. Van Raamsdonk CD, Fitch KR, Fuchs H, de Angelis MH, Barsh GS. Effects of G-protein mutations on skin color. *Nat Genet*. 2004;36:961–968.
34. Gao C, Wang Y, Broaddus R, Sun L, Xue F, Zhang W. Exon 3 mutations of *CTNNB1* drive tumorigenesis: a review. *Oncotarget*. 2018;9:5492–5508.
35. Rubinfeld B, Souza B, Albert I, et al. Association of the *APC* gene product with β-catenin. *Science*. 1993;262:1731–1734.
36. Rubinfeld B, Albert I, Porfiri E, Fiol C, Munemitsu S, Polakis P. Binding of GSK3β to the APC-β-catenin complex and regulation of complex assembly. *Science*. 1996;272:1023–1026.
37. Korinek V, Barker N, Morin PJ, et al. Constitutive transcriptional activation by a β-catenin-Tcf complex in APC$^{-/-}$ colon carcinoma. *Science*. 1997;275:1784–1787.
38. Morin PJ, Sparks AB, Korinek V, et al. Activation of β-catenin-Tcf signaling in colon cancer by mutations in β-catenin or APC. *Science*. 1997;275:1787–1790.
39. Kongkanuntn R, Bubb VJ, Sansom OJ, Wyllie AH, Harrison DJ, Clarke AR. Dysregulated expression of β-catenin marks early neoplastic change in *Apc* mutant mice, but not all lesions arising in *Msh2* deficient mice. *Oncogene*. 1999;18:7219–7225.
40. Kavela S, Shinde SR, Ratheesh R, et al. PNUTS functions as a proto-oncogene by sequestering PTEN. *Cancer Res*. 2013;73:205–214.
41. Dingar D, Tu WB, Resetca D, et al. MYC dephosphorylation by the PP1/PNUTS phosphatase complex regulates chromatin binding and protein stability. *Nat Commun*. 2018;9:3502.
42. Marx A, Luebke AM, Clauditz TS, et al. Upregulation of phosphatase 1 nuclear-targeting subunit (PNUTS) is an independent predictor of poor prognosis in prostate cancer. *Dis Markers*. 2020;2020:7050146.
43. Lin YH, Zhen YY, Chien KY, et al. LIMCH1 regulates nonmuscle myosin-II activity and suppresses cell migration. *Mol Biol Cell*. 2017;28:1054–1065.
44. Zhang Y, Zhang Y, Xu H. LIMCH1 suppress the growth of lung cancer by interacting with HUWE1 to sustain p53 stability. *Gene*. 2019;712:143963.
45. Cao H, Zhao J, Chen Z, et al. Loss of LIMCH1 predicts poor prognosis in patients with surgically resected lung adenocarcinoma: a study based on immunohistochemical analysis and bioinformatics. *J Cancer*. 2021;12:181–189.
46. Wu JN, Roberts CW. *ARID1A* mutations in cancer: another epigenetic tumor suppressor? *Cancer Discov*. 2013;3:35–43.
47. Jiang T, Chen X, Su C, Ren S, Zhou C. Pan-cancer analysis of *ARID1A* alterations as biomarkers for immunotherapy outcomes. *J Cancer*. 2020;11:776–780.
48. van de Nes J, Gessi M, Sucker A, et al. Targeted next generation sequencing reveals unique mutation profile of primary melanocytic tumors of the central nervous system. *J Neurooncol*. 2016;127:435–444.
49. Thielmann CM, Matull J, Roth S, et al. Genetic and clinical characteristics of *ARID1A* mutated melanoma reveal high tumor mutational load without implications on patient survival. *Cancers (Basel)*. 2022;14:2090.
50. Koo BK, Spit M, Jordens I, et al. Tumour suppressor RNF43 is a stem-cell E3 ligase that induces endocytosis of Wnt receptors. *Nature*. 2012;488:665–669.
51. Hao HX, Xie Y, Zhang Y, et al. ZNRF3 promotes Wnt receptor turnover in an R-spondin-sensitive manner. *Nature*. 2012;485:195–200.
52. de Lau W, Peng WC, Gros P, Clevers H. The R-spondin/Lgr5/Rnf43 module: regulator of Wnt signal strength. *Genes Dev*. 2014;28:305–316.
53. Giannakis M, Hodis E, Jasmine Mu X, et al. RNF43 is frequently mutated in colorectal and endometrial cancers. *Nat Genet*. 2014;46:1264–1266.
54. Wang K, Yuen ST, Xu J, et al. Whole-genome sequencing and comprehensive molecular profiling identify new driver mutations in gastric cancer. *Nat Genet*. 2014;46:573–582.
55. Seeber A, Battaglin F, Zimmer K, et al. Comprehensive analysis of R-spondin fusions and RNF43 mutations implicate novel therapeutic options in colorectal cancer. *Clin Cancer Res*. 2022;28:1863–1870.
56. Elez E, Ros J, Fernández J, et al. *RNF43* mutations predict response to anti-BRAF/EGFR combinatory therapies in *BRAF*^{V600E} metastatic colorectal cancer. *Nat Med*. 2022;28:2162–2170.

Investigative Ophthalmology & Visual Science

57. Fang L, Ford-Roshon D, Russo M, et al. *RNF43* G659fs is an oncogenic colorectal cancer mutation and sensitizes tumor cells to PI3K/mTOR inhibition. *Nat Commun*. 2022;13:3181.
58. Stevanin G, Santorelli FM, Azzedine H, et al. Mutations in *SPG11*, encoding spatacsin, are a major cause of spastic paraplegia with thin corpus callosum. *Nat Genet*. 2007;39:366–372.
59. Paisan-Ruiz C, Dogu O, Yilmaz A, Houlden H, Singleton A. *SPG11* mutations are common in familial cases of complicated hereditary spastic paraplegia. *Neurology*. 2008;70:1384–1389.
60. Kara E, Tucci A, Manzoni C, et al. Genetic and phenotypic characterization of complex hereditary spastic paraplegia. *Brain*. 2016;139:1904–1918.
61. Schüle R, Wiethoff S, Martus P, et al. Hereditary spastic paraplegia: clinicogenetic lessons from 608 patients. *Ann Neurol*. 2016;79:646–658.
62. Dogrusöz M, Ruschel Trasel A, Cao J, et al. Differential expression of DNA repair genes in prognostically-favorable versus unfavorable uveal melanoma. *Cancers (Basel)*. 2019;11:1104.

Investigative Ophthalmology & Visual Science